Supplementary Information

A Transparent and Robust Ionogel Prepared via Phase Separation for Sensitive Strain Sensing

*Jinliang Xie[1&], Xiaoqian Li[2&], Jiayu Liu[1], Fangfang Su[1], Ruiqi Gao[3], Changming Zhang[3], Jiahe Liang[2], Gang Ji[*3], Dongdong Yao[*1], Yaping Zheng[1]*

[1] School of Chemistry and Chemical Engineering, Northwestern Polytechnical University Xi'an, Shaanxi 710072, P. R. China;

[2] 3D Printing Research Center, Department of Ultrasonic Medicine, Tang Du Hospital, Air Force Medical University, No.569 of Xin Si Road, Xi'an, Shaanxi 710038. P. R. China.

[3] Department of Digestive Surgery, Xijing Hospital, Air Force Medical University, Xi'an, Shaanxi 710032. P. R. China.

[*] Corresponding authors. E-mail: yaodd@nwpu.edu.cn (Dongdong Yao), jigang@fmmu.edu.cn (Gang Ji).

Table of Contents

Figure S5. Viscosity-frequency curves of the precursor solution.

Figure S6. The tensile stress-strain curves of P(DMAAm$_{40}$-*co*-AM$_{60}$) ionogel after being placed in different relative humidity environments for 24 hours.

Figure S7. The conductivity of P(DMAAm$_{40}$-*co*-AM$_{60}$) ionogel after being placed in different relative humidity environments for 24 hours.

Figure S8. The process of programmed box-shaped P(DMAAm$_{40}$-*co*-AM$_{60}$) ionogel regaining its initial shape under heating conditions.

Figure S9. Photographs of E. coli bacterial colonies upon treatment with P(DMAAm$_{x}$-*co*-AM$_{y}$) ionogel.

3. Supplementary tables

Table S1. Transparency and characteristic temperature of the P(DMAAm$_{x}$-*co*-AM$_{y}$) ionogels.

Table S2. Mechanical properties of the P(DMAAm$_{x}$-*co*-AM$_{y}$) ionogels.

Table S3. The mechanical properties of reported high strength gel materials.

Table S4. Tensile properties and conductivity of P(DMAAm$_{40}$-*co*-AM$_{60}$) ionogel under different humidity environments.

Table S5. Comparison of sensing performance of gel-based flexible strain sensors.

4. Reference

Supplementary Note 1

Antibacterial activity: E. coli (ATCC25922, Gram-negative) were used to evaluate the antibacterial performances of the composite ionogels. Bacteria were cultured in Luria-Bertani (LB) broth at 37 °C, with continuous shaking at 150 rpm overnight, and then diluted for further use. Briefly, 100 μL bacterial suspension (10^5 CFU/mL) was spread on the agar plate, followed by the addition of the composite ionogels and incubation at 37 °C for 24 h. Subsequently, the agar plate was incubated at 37 °C for 24 h and then the diameter of the inhibition zone around the hydrogel was measured.

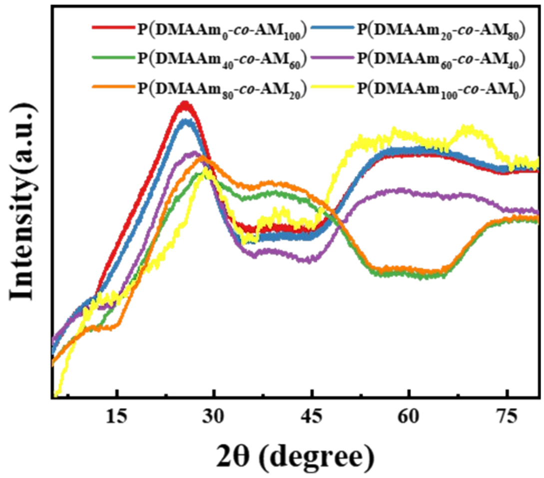

Figure S1. The XRD curves of the P(DMAAm$_x$-*co*-AM$_y$) ionogels.

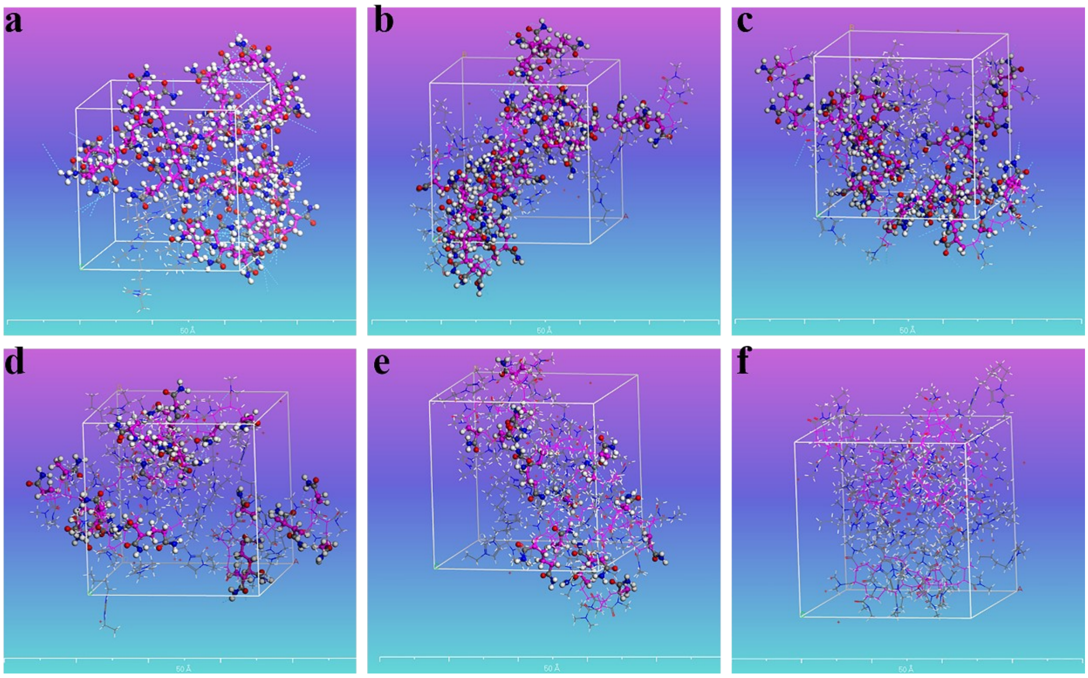

Figure S2. Structure models of P(DMAAm$_x$-*co*-AM$_y$) ionogels with anneal and dynamic optimized based on MD calculation. (a) P(DMAAm$_0$-*co*-AM$_{100}$) ionogel, (b) P(DMAAm$_{20}$-*co*-AM$_{80}$) ionogel, (c) P(DMAAm$_{40}$-*co*-AM$_{60}$) ionogel, (d) P(DMAAm$_{60}$-*co*-AM$_{40}$) ionogel, (e) P(DMAAm$_{80}$-*co*-AM$_{20}$) ionogel, (f) P(DMAAm$_{100}$-*co*-AM$_0$) ionogel.

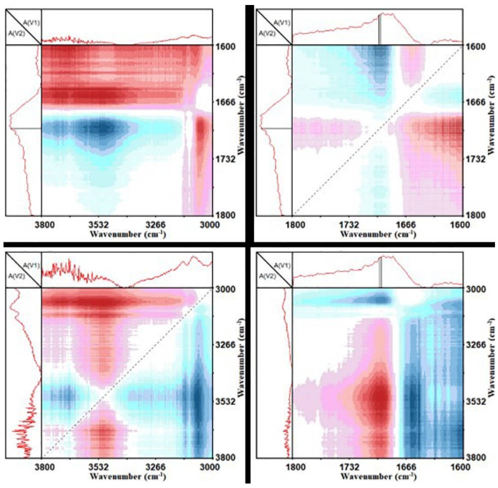

Figure S3. 2D correlation asynchronous spectra of the P($DMAAm_{40}$-*co*-AM_{60}) ionogel.

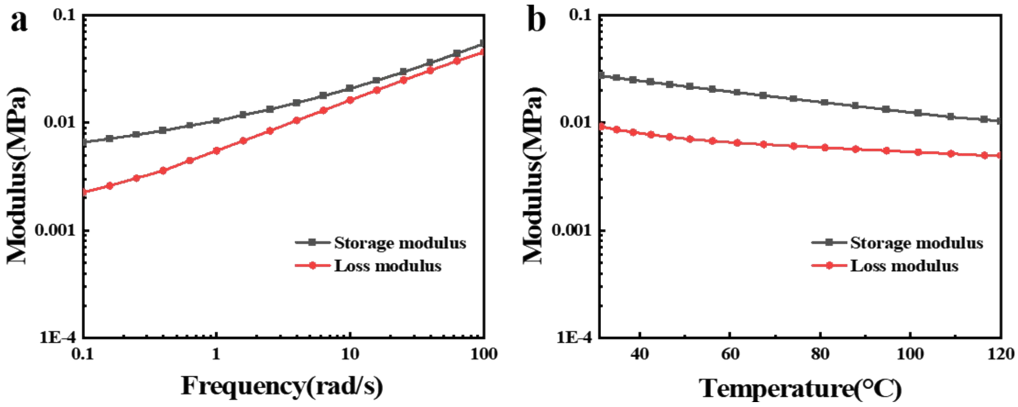

Figure S4. Rheology analyses of P($DMAAm_{40}$-*co*-AM_{60}) ionogel. (a) Modulus-frequency relationship curves, (b) Modulus-temperature relationship curves.

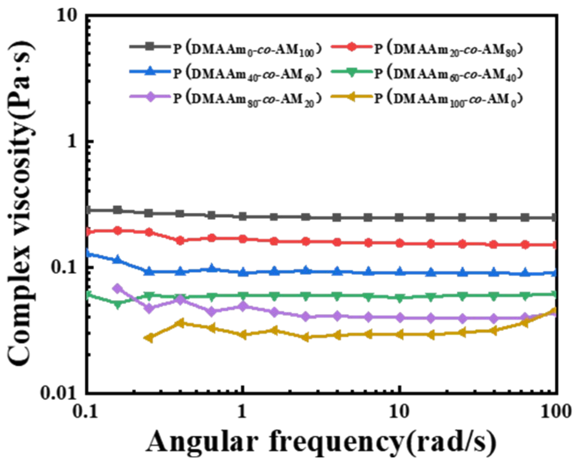

Figure S5. Viscosity-frequency curves of the precursor solution.

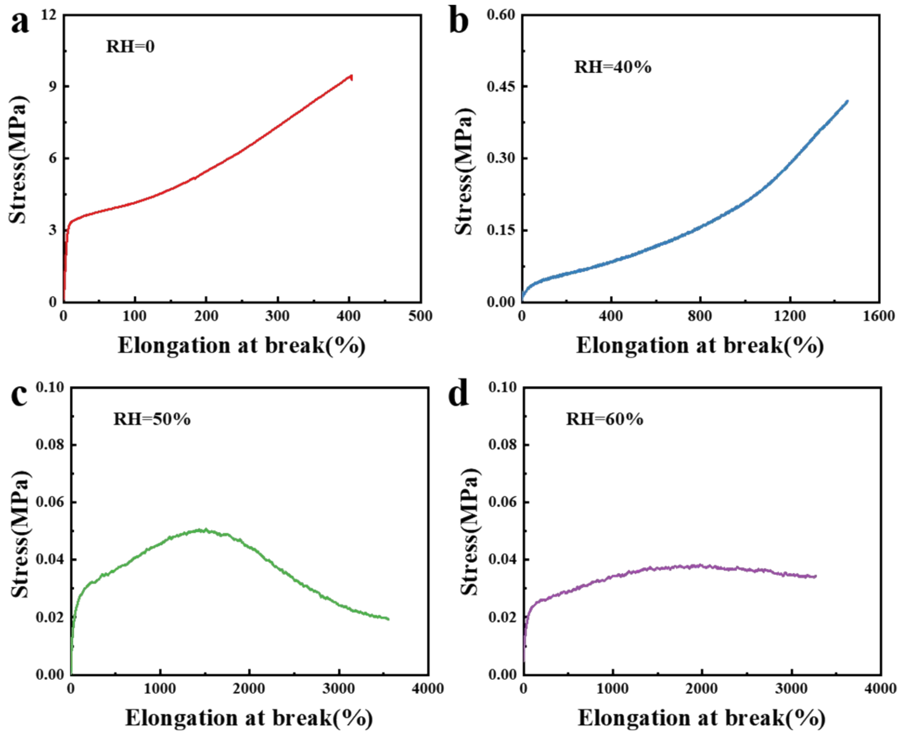

Figure S6. The tensile stress-strain curves of P(DMAAm$_{40}$-*co*-AM$_{60}$) ionogel after being placed in different relative humidity environments for 24 hours, (a) dry environment, (b) 40%, (c) 50%, (d) 60%.

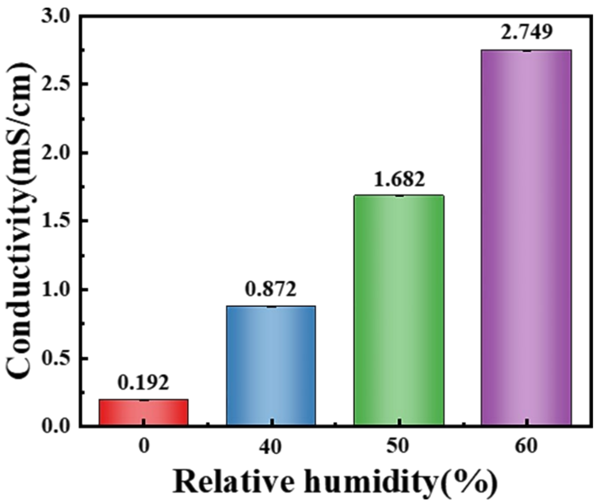

Figure S7. The conductivity of P(DMAAm40-co-AM60) ionogel after being placed in different relative humidity environments for 24 hours.

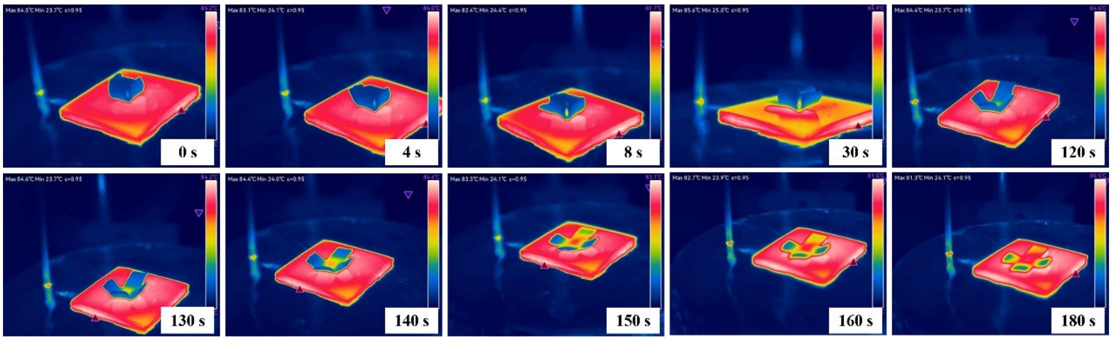

Figure S8. The process of programmed box-shaped P($DMAAm_{40}$-*co*-AM_{60}) ionogel regaining its initial shape under heating conditions.

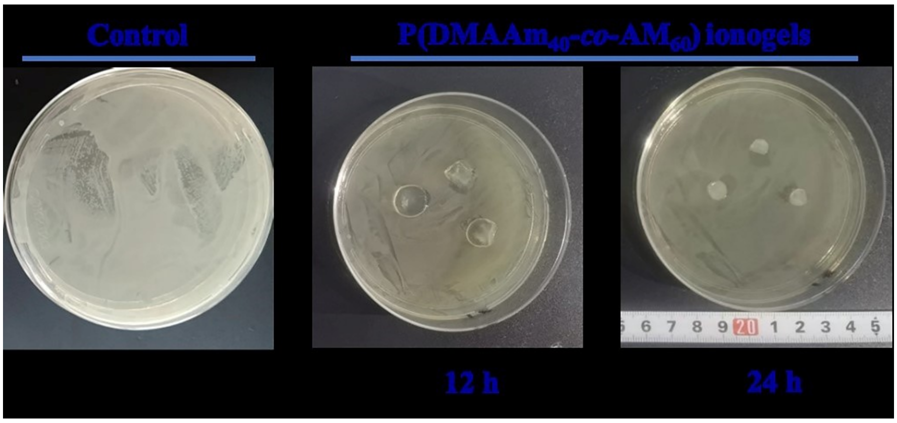

Figure S9. Photographs of E. coli bacterial colonies upon treatment with P($DMAAm_x$-*co*-AM_y) ionogel.

Additionally, E. coli (ATCC25922, Gram-negative) were used to evaluate the antibacterial performances of the P($DMAAm_{40}$-*co*-AM_{60}) ionogel. The ionogel samples of a certain volume were placed onto solid nutrient agar coated with a suspension of E. coli bacteria at 37 °C for 12 hours and 24 h. However, the ionogel have no obvious antibacterial properties.

Table S1. Transparency and characteristic temperature of the P(DMAAm$_x$-*co*-AM$_y$) ionogels.

Sample	Transparency (%)	T_g (°C) [a]	T_d (°C) [b]	$T_{d\ fast}$ (°C) [c]
P(DMAAm$_0$-*co*-AM$_{100}$)	89.6	>60	263	311
P(DMAAm$_{20}$-*co*-AM$_{80}$)	90.5	50.7	263	318
P(DMAAm$_{40}$-*co*-AM$_{60}$)	94.0	26.2	263	310
P(DMAAm$_{60}$-*co*-AM$_{40}$)	95.2	9.4	263	315
P(DMAAm$_{80}$-*co*-AM$_{20}$)	96.5	-2.2	263	321
P(DMAAm$_{100}$-*co*-AM$_0$)	98.3	<-40	263	311

a. T_g represents the glass transition temperature; b. T_d represents the decomposition temperature; c. $T_{d\ fast}$ represents the fastest decomposition temperature.

Table S2. Mechanical properties of the P(DMAAm$_x$-*co*-AM$_y$) ionogels.

Sample	Tensile strength (MPa)	Elongation at break (%)	Modulus (MPa)	Toughness (MJ/m^3)
P(DMAAm$_0$-*co*-AM$_{100}$)	11.83	6.82	152.70	0.56
P(DMAAm$_{20}$-*co*-AM$_{80}$)	9.07	297.07	127.83	21.46
P(DMAAm$_{40}$-*co*-AM$_{60}$)	8.94	404.46	51.55	21.95
P(DMAAm$_{60}$-*co*-AM$_{40}$)	5.55	614.18	5.44	15.44
P(DMAAm$_{80}$-*co*-AM$_{20}$)	2.25	1262.10	0.31	11.64
P(DMAAm$_{100}$-*co*-AM$_0$)	0.113	1319.06	0.0245	0.65

Table S3. The mechanical properties of reported high strength gel materials.

No.	Strength (MPa)	Modulus (MPa)	Toughness ($MJ\cdot m^{-3}$)	Type
1	3.64	0.46	27.60	Hydrogel[1]
2	5.60	1.30	--	Hydrogel[2]
3	3.10	0.60	8.65	Hydrogel[3]
4	1.36	0.49	--	Hydrogel[4]
5	2.00	--	22.00	Hydrogel[5]
6	2.70	1.17	10.80	Hydrogel[6]
7	2.20	0.27	--	Hydrogel[7]
8	2.70	0.82	8.50	Hydrogel[8]
9	9.30	277.00	0.40	Hydrogel[9]
10	20.20	16.10	62.70	DES gel[10]
11	3.19	2.35		DES gel [11]
12	5.19	0.20	--	PU-IL ionogel[12]
13	2.52	1.43	2.55	PU-IL ionogel[13]
14	22.00	--	109.80	PU-IL ionogel[14]
15	4.99	1.71	--	PU-IL ionogel[15]
16	1,65	0.28	--	PU-IL ionogel [16]
17	9.15	1.12	178.46	BC ionogel[17]
18	3.70	2.46	6.25	Organic-inorganic ionogel[18]
19	0.23	0.04	--	PILs ionogel[19]
20	2.28	2.28	--	PILs ionogel[20]
21	15.00	82.81	--	PILs ionogel[21]
22	12.60	46.50	--	P(AA-*co*-AM) ionogel[22]
23	7.12	0.94	--	P(IBA-*co*-MEA) ionogel[23]
24	0.37	0.42	21.80	PAA/CNF ionogel[24]
25	14.30	55.00	78.00	PDMAA ionogel[25]
26	0.90	15.60	2.48	PSHM ionogel[26]
27	4.80	0.48	--	PEA ionogel[27]
28	7.60	58.00	25.00	PDMAA/MOF ionogel[28]
29	5.00	--	7.40	P(AA-*co*-HFBA) ionogel [29]
30	0.80	1.05	5.52	P(AA-*co*-ZDMA) ionogel [30]
31	11.70	72.20	37.50	PVDF-*co*-HFP ionogel [31]
32	4.70	--	--	BP@PVP ionogel [32]
33	21.00	325.00	102	P(AA-*co*-AM)/Zn^{2+} ionogel [33]

Table S4. Tensile properties and conductivity of P(DMAAm$_{40}$-*co*-AM$_{60}$) ionogel under different humidity environments.

Humidity (%)	**Tensile strength (MPa)**	**Elongation at break (%)**	**Conductivity (mS·cm^{-1})**
0	8.94	404.46	0.192
40	0.420	1456	0.872
50	0.051	>3500	1.682
60	0.038	>3300	2.749

Gel	Stretchability		Gauge factor	Ref.
	Tensile strain	Tensile strength(kPa)		
PAM/SF/GO/PEDOT:PSS hydrogel	600%	N/A	0.8(0–50%) 1.6(50-400%) 0.6(400%-600%)	34
GA/rGO/PAM hydrogel	2094%	118.7	2.496(0–40%) 3.957(40–100%) 15.467(100–1000%)	35
PVA-G-PDA-AgNPs hydrogel	331%	1174	0.937(0–70%) 0.13(>70%)	36
PAA/CS/GO/Gly hydrogel	>1000%	N/A	1.138(0–80%) 4.7(>80%)	37
PAA/PDA-rGO/Fe^{3+} hydrogel	>600%	400	1.32(100–500%)	38
PVA/SA/MXene hydrogel	263%	~100	0.97(0-100%)	39
MXene nanocomposite organohydrogel	~1000%	~50	5.02(0-200%) 44.85(200-350%)	40
PAM/carrageenan/Eg/Gl organohydrogel	N/A	N/A	1.9(0-200%) 6(250-400%)	41
P(AA-*co*-AM)/PDA-CNTs/Gl organohydrogel	~800	~50	N/A	42
PVA/DMSO/rGO/GO organohydrogel	~600%	3100	2.21(0–600%)	43
PVA/PEDOT:PSS organohydrogel	~700%	~2100	N/A	44
PVA/PANI organohydrogel	458%	477	2.14(0-100%)	45
P(VDF-*co*-HFP)/P(MMA-*co*-BMA) ionogel	307%	2310	1.62(0-150%)	46
P(MEA-*co*-MTMA/TFSI) ionogel	1440%	1100	0-7.3(0-400%)	47
P(MEA-*co*-IBA) ionogel	1400%	7120	2.02（1%） 2.02-4(1-100%) 4-6(100-200%)	23
PAA/CNF/IL/H_2O ionogel	11760%	~200	0-9.8(0-2000%)	24
PDMAA/Zn^{2+} ionogel	N/A	14300	2.8(0-200%) 6.2(250-600%) 9.2(600-900%)	25
P(DMAAm-*co*-AM) ionogel	**404%**	**8940**	**2.73(0-10%)** **0.67(10-200%)**	**This work**

Table S5. Comparison of sensing performance of gel-based flexible strain sensors.

Reference

1. N. Yuan, L. Xu, H. Wang, Y. Fu, Z. Zhang, L. Liu, C. Wang, J. Zhao and J. Rong, *ACS Appl. Mater. Inter.*, 2016, **8**, 34034-34044.
2. Y. Yang, X. Wang, F. Yang, L. Wang and D. Wu, *Adv. Mater.*, 2018, **30**, 1707071.
3. S. X. Pan, M. Xia, H. H. Li, X. L. Jiang, P. X. He, Z. G. Sun and Y. H. Zhang, *J. Mater. Chem. C*, 2020, **8**, 2827-2837.
4. S. H. Li, H. Y. Pan, Y. T. Wang and J. Q. Sun, *J. Mater. Chem. A*, 2020, **8**, 3667-3675.
5. T. Nakajima, Y. Fukuda, T. Kurokawa, T. Sakai, U. I. Chung and J. P. Gong, *ACS Macro Lett.*, 2013, **2**, 518-521.
6. L. J. Zhou, X. J. Pei, K. Fang, R. Zhang and J. Fu, *Polymer*, 2020, **192**, 122319.
7. J. Wen, X. Zhang, M. Pan, J. Yuan, Z. Jia and L. Zhu, *Polymers*, 2020, **12**, (1), 239.
8. Y. Zhang, M. Y. Li, X. Han, Z. W. Fan, H. H. Zhang and Q. L. Li, *Chem. Phys. Lett.*, 2021, **769**, 138437.
9. H. P. Yu and Y. J. Zhu, *Nano Res.*, 2021, **14**, 3643-3652.
10. H. Zhang, N. Tang, X. Yu, M. H. Li and J. Hu, *Adv. Funct. Mater.*, 2022, **32**, 2206305.
11. Q. Wu, S. Han, J. Zhu, A. Chen, J. Zhang, Z. Yan, J. Liu, J. Huang, X. Yang and L. Guan, *Chem. Eng. J.*, 2023, **454**, 140328.
12. M. W. Zhang, R. Yu, X. L. Tao, Y. Y. He, X. P. Li, F. Tian, X. Y. Chen and W. Huang, *Adv. Funct. Mater.*, 2022, **33**, 2208083.
13. T. Li, Y. Wang, S. Li, X. Liu and J. Sun, *Adv. Mater.*, 2020, **32**, 2002706.
14. P. Liu, D. F. Pei, Y. P. Wu, M. J. Li, X. H. Zhao and C. X. Li, *J. Mater. Chem. A*, 2022, **10**, 25602-25610.
15. H. Wang, J. Xu, K. Li, Y. Dong, Z. Du and S. Wang, *J Mater. Chem. B*, 2022, **10**, 1301-1307.
16. L. Yang, L. Sun, H. Huang, W. Zhu, Y. Wang, Z. Wu, R. E. Neisiany, S. Gu and Z. You, *Adv Sci*, 2023, **10**, 2207527.
17. G. D. Fan, K. K. Liu, H. Su, Y. Q. Luo, Y. Geng, L. Y. Chen, B. J. Wang, Z. P. Mao, X. F. Sui and X. L. Feng, *Chem. Eng. J.*, 2022, **434**, 134702.
18. L. Yu, S. Guo, Y. Lu, Y. Li, X. Lan, D. Wu, R. Li, S. Wu and X. Hu, *Adv. Energy Mater.*, 2019, **9**, 1900257.
19. Y. Zhao, D. L. Gan, L. C. Wang, S. Y. Wang, W. J. Wang, Q. Wang, J. J. Shao and X. C. Dong, *Adv. Mater. Tech.*, 2023, **8**, 2201566.
20. Y. Ren, J. Guo, Z. Liu, Z. Sun, Y. Wu, L. Liu and F Yan. Sci. Adv., 2019, **5**, 0648.
21. Z. Yu and P. Wu, *Adv. Mater.*, 2021, **33**, 2008479.
22. M. Wang, P. Zhang, M. Shamsi, J. L. Thelen, W. Qian, V. K. Truong, J. Ma, J. Hu and M. D. Dickey, *Nat. Mater.*, 2022, **21**, 359-365.
23. B. Yiming, Y. Han, Z. Han, X. Zhang, Y. Li, W. Lian, M. Zhang, J. Yin, T. Sun, Z. Wu, T. Li, J. Fu, Z. Jia and S. Qu, *Adv. Mater.*, 2021, **33**, 2006111.
24. Y. H. Ye, H. Oguzlu, J. Y. Zhu, P. H. Zhu, P. Yang, Y. L. Zhu, Z. M. Wan, O. J. Rojas and F. Jiang, *Adv. Funct. Mater.*, 2023, **33**, 2209787.
25. L. Li, W. Li, X. Wang, X. Zou, S. Zheng, Z. Liu, Q. Li, Q. Xia and F. Yan, *Angew. Chem. Int. Ed. Engl.*, 2022, **61**, e202212512.

26. K. G. Cho, S. An, D. H. Cho, J. H. Kim, J. Nam, M. Kim and K. H. Lee, *Adv. Funct. Mater.*, 2021, **31**, 2102386.
27. Z. Q. Cao, H. L. Liu and L. Jiang, *Mater. Horiz.*, 2020, **7**, 912-918.
28. Q. Xia, W. Li, X. Zou, S. Zheng, Z. Liu, L. Li and F. Yan, *Mater Horiz*, 2022, **9**, 2881-2892.
29. J. Chen, Y. Wang, L. Li, Y. E. Miao, X. Zhao, X. P. Yan, C. Zhang, W. Feng and T. Liu, *ACS Appl. Mater. Inter.*, 2023, **15**, 16109-16117.
30. S. Hao, C. Yang, X. Yang, T. Li, L. Ma, Y. Jiao and H. Song, *ACS Appl. Mater. Inter.*, 2023, **15**, 16132-16143.
31. W. Q. Zhan, H. Q. Zhang, X. Lyu, Z. Z. Luo, Y. Yu and Z. G. Zou, *Sci. China Mater.*, 2023, **66**, 1539-1550.
32. X. F. Xiao, H. D. Zhao, P. J. Yan, H. F. Zhang, X. H. Liu, X. Jia and S. P. Jin, *J. Mater. Chem. A*, 2023, **11**, 6616-6626.
33. Z. K. Huang, Y. T. Chen, J. P. Peng, T. R. Huang, F. Q. Hu, X. Liu, L. G. Xu and K. Yue, *J. Mater. Chem. A*, 2023, **11**, 7201-7212.
34. F. He, X. You, H. Gong, Y. Yang, T. Bai, W. Wang, W. Guo, X. Liu and M. Ye, *ACS Appl. Mater. Inter.*, 2020, **12**, 6442-6450.
35. X. Zheng, Y. Gao, X. Ren and G. Gao, *J Mater. Chem. C*, 2021, **9**, 3343-3351.
36. L. Fan, J. Xie, Y. Zheng, D. Wei, D. Yao, J. Zhang and T. Zhang, *ACS Appl. Mater. Inter.*, 2020, **12**, 22225-22236.
37. S. Xia, S. Song, Y. Li and G. Gao, *J Mater. Chem. C*, 2019, **7**, 11303-11314.
38. X. Jing, H. Y. Mi, X. F. Peng and L. S. Turng, *Carbon*, 2018, **136**, 63-72.
39. T. Wang, J. Wang, Z. Li, M. Yue, X. Qing, P. Zhang, X. Liao, Z. Fan and S. Yang, *J Appl. Polym. Sci.*, 2021, **139,** 51627.
40. H. Liao, X. L. Guo, P. B. Wan and G. H. Yu, *Adv. Funct. Mater.*, 2019, **29**, 1904507.
41. J. Wu, Z. Wu, X. Lu, S. Han, B. R. Yang, X. Gui, K. Tao, J. Miao and C. Liu, *ACS Appl. Mater. Inter.*, 2019, **11**, 9405-9414.
42. L. Han, K. Liu, M. Wang, K. Wang, L. Fang, H. Chen, J. Zhou and X. Lu, *Adv. Funct. Mater.*, 2017, **28,** 1704195.
43. H. Chen, J. Huang, J. Liu, J. Gu, J. Zhu, B. Huang, J. Bai, J. Guo, X. Yang and L. Guan, *J. Mater. Chem. A*, 2021, **9**, 23243-23255.
44. Q. Rong, W. Lei, L. Chen, Y. Yin, J. Zhou and M. Liu, *Angew. Chem. Int. Ed. Engl.*, 2017, **56**, 14159-14163.
45. C. X. Hu, Y. L. Zhang, X. D. Wang, L. Xing, L. Y. Shi and R. Ran, *ACS Appl. Mater. Inter.*, 2018, **10**, 44000-44010.
46. J. Lan, Y. Li, B. Yan, C. Yin, R. Ran and L.-Y. Shi, *ACS Appl. Mater. Inter.*, 2020, **12**, 37597-37606.
47. C. He, S. Sun and P. Wu, *Mater. Horiz.*, 2021, **8**, 2088-2096.